

Genuine multipartite entanglement in superconducting phases of doped quantum spin ladders

Sudipto Singha Roy, Himadri Shekhar Dhar, Debraj Rakshit, Aditi Sen(De), and Ujjwal Sen
Harish-Chandra Research Institute, Chhatnag Road, Jhansi, Allahabad 211 019, India

(Dated: October 28, 2022)

We investigate the trends of genuine multipartite entanglement of high-temperature superconducting states, usually described by doping the Mott insulator. We begin by analyzing the ground states of a Hubbard model with large onsite interactions obtained by exact diagonalization in regimes where the superconducting phase is observed for relatively high doping. The ground states are observed to be genuine multipartite entangled, with the maximum value achieved close to the superconducting phase boundary. Subsequently, for finite hole doping, the short-range resonating valence bond (RVB) state is considered to be the ground state of the Hubbard model. We prove that doped RVB ladder states are always genuine multipartite entangled. We then formulate an analytical recursion method for the wave function, which allows us to efficiently estimate the entanglement as well as other physical quantities in large doped RVB ladders. The maximum genuine multipartite entanglement in these RVB states is observed at doping corresponding to the superconducting phase of the Hubbard model.

Introduction.—The discovery of high-temperature (T_c) superconductivity [1–5] has been one of the hallmarks of modern physics with significant impact on our understanding of strongly-correlated systems and potential application in path-breaking technologies [6], from particle accelerators [7] to superconducting quantum interference devices (SQUIDs) [8]. Most developments in high- T_c superconductivity involve antiferromagnetic order in doped Mott insulators [9] based on transition-metal oxides [3, 4], as compared to the more conventional superconductivity [10] at low temperatures based on the BCS theory [11] (cf. [12–14]). Over the years, notable progress has been made in experimental investigation of high- T_c superconductivity [15] but the microscopic theory behind this novel phenomenon remains unresolved [16].

One of the best known and simplest theoretical frameworks for investigating high- T_c superconductivity is the t - J ladder [17, 18], which is obtained in the limit of large on-site interaction from the Hubbard model [19]. At half-filling, without doping, the system reduces to a Heisenberg ladder with a spin liquid ground state (GS) [20]. Upon doping the t - J ladder, studies based on mean-field theory using Gutzwiller renormalization show that the spin gap is persistent [21], which is a tell-tale sign of strong superconducting fluctuations [20–22]. The superconducting states of the t - J ladder can be represented using the short-range resonating valence bond (RVB) ansatz [23, 24], which were introduced to describe Mott-insulators in spin-1/2 Heisenberg antiferromagnets (AFMs) [24]. The RVB state is a possible GS of the half-filled t - J ladder [25] and, upon finite doping, provides a simple mechanism to describe high- T_c superconductivity [2–4]. Considerable work has been done along these directions to formulate a plausible theory of high- T_c superconductivity [17–26], while countercurrents remain [16, 27].

In recent years, entanglement [28] has been found to be an efficient indicator of several interesting phenomena in strongly-correlated systems [29], ranging from quantum phase transitions [30] to topological order [31]. In particular cases, multipartite entanglement turns out to be more effective compared to bipartite measures in understanding cooperative properties in complex many-body systems [32], including

spin liquids such as RVB states [33–37].

In this work, we investigate the behavior of genuine multipartite entanglement of the GS of doped t - J ladder Hamiltonian. We consider the J/t regime where the superconducting phases occur for relatively high “hole” (vacant lattice site) doping concentration [38]. To formulate the problem, we treat the hole-spin composite unit as a three-level system or a qutrit. The GS of the t - J ladder is obtained through exact diagonalization and the genuine multiparty entanglement is measured using the generalized geometric measure (\mathcal{G}) [39] (cf. [40]), for a range of the electron density ($n_{el} = k/N$), where $2N$ and $2k$ are the number of sites and electrons in the ladder. For a fixed lattice of $2N$ sites, we observe that \mathcal{G} of the GS of the t - J ladder increases with n_{el} , reaching a maximum at $n_c \approx 0.65$ before decreasing for higher n_{el} . The value n_c corresponds to the phase where superconducting correlations occur for $J/t \approx 0.6$ [38]. We next consider the short-range RVB states as a possible basis to study GS of the t - J model. For finite values of the electron density, n_{el} , and using the symmetry properties of doped RVB states [35, 36], we prove that the doped RVB ladder is always genuinely multipartite entangled. To obtain \mathcal{G} in large ladders, where exact calculations are inaccessible, we introduce an analytical recursion method to build the hole-RVB GS and its reduced density matrices. Using this analytical method, we observe that \mathcal{G} increases with n_{el} and reaches a maximum at n_c predicted by numerical results of the finite-sized t - J ladder in the superconducting phase. Hence, the maximum genuine multipartite entanglement in doped RVB ladders corresponds to the strongly-correlated superconducting phase of the t - J model. One should note that although we use the recursion method to study multipartite entanglement, the method can also be employed to investigate other properties like single-site, two-site physical quantities of the doped RVB ladders for systems with an arbitrary number of sites. In our calculations, we have considered up to 300 sites, with the physical quantities of interest having converged much before.

Model.—We begin with a quantum spin-1/2 ladder system, consisting of an arbitrary numbers of holes and spin particles, described by the t - J Hamiltonian. The model can be derived

using second order perturbation theory of the Hubbard model at the limit of large on-site interaction [19, 41–43]. The t - J Hamiltonian on a ladder can be written as

$$\mathcal{H} = -t \sum_{\langle i,j \rangle, \sigma} \mathcal{P}_G (c_{i\sigma}^\dagger c_{j\sigma} + \text{h.c.}) \mathcal{P}_G + J \sum_{\langle i,j \rangle} \vec{S}_i \cdot \vec{S}_j, \quad (1)$$

where $c_{i\sigma}$ ($c_{i\sigma}^\dagger$) is the fermionic annihilation (creation) operator of spin σ ($= \{\uparrow, \downarrow\}$), and \vec{S}_i is the triad of spin-1/2 operators, at site i . The Heisenberg exchange coupling (J) is isotropic along the rungs and legs while t represents the transfer energy and the expression $\langle i, j \rangle$ denotes that the sum is taken over nearest neighbor (NN) sites. \mathcal{P}_G is the Gutzwiller projector $\Pi_i(1 - n_{i\uparrow}n_{i\downarrow})$ which enforces at most single occupancy at each lattice site. This ensures that the undoped state physically represents a Mott insulator. The t - J model, under finite doping, exhibits a rich phase diagram, which has been extensively studied for low-dimensional antiferromagnets (AFM) [38, 44–46]. In particular, the t - J model in 1D and ladder configurations possess exotic correlation properties that are characterized by the Luttinger liquid theory [47], as confirmed using exact diagonalization calculations, and exhibits a rich superconducting phase for a specific range of values of J/t and electron density, n_{el} [3, 4, 44–46]. In this work, our interest lies in investigating t - J ladders in the region $J/t \gtrsim 0.5$ where the superconducting phase seems to appear at relatively high n_{el} [38]. This is also influenced by the fact that these J/t regimes can potentially be realized in fermionic ultracold gases at high energy scales [48]. An important approach to analyze the t - J Hamiltonian, beyond exact diagonalization, is to consider RVB spin liquid GS, which is supported by various numerical simulations [49]. Under the ansatz, the RVB state is defined as the equal-weight superposition of all possible short-range (NN) dimer coverings and were introduced as the Mott insulator phase in an AFM [24], which under finite doping exhibits an insulator-superconductor transition [2]. Using the doped RVB, we first compare its multipartite entanglement properties with those obtained from exact diagonalization of the t - J model, for moderate-sized ladders, and find a qualitative agreement between the two. We subsequently investigate the multipartite entanglement properties of superconducting strongly correlated fermions on large ladders within the doped RVB ansatz, via the analytical method described here for this purpose.

Let us consider the doped RVB state containing $2N$ lattice sites, on a ladder configuration, with $2k$ spin-1/2 particles and $2(N - k)$ holes or vacant lattice sites, expressed using a *bipartite lattice*, consisting of sublattices A and B . The corresponding (unnormalized) wavefunction, with electron density $n_{el} = k/N$, is given by

$$|\Psi\rangle_{k,N-k} = \sum_i r_i |(a_{n_1} b_{n_1})(a_{n_2} b_{n_2}) \cdots (a_{n_k} b_{n_k})\rangle_i \otimes |h_{m_{2k+1}} h_{m_{2k+2}} \cdots h_{m_{2N}}\rangle_i, \quad (2)$$

where $|(a_{n_j} b_{n_j})\rangle = \frac{1}{\sqrt{2}}(|01\rangle - |10\rangle)_{n_j}$ represents a dimer, with $a_j \in A$ and $b_j \in B$. $|\{(a_{n_j} b_{n_j})\}\rangle_i$ represents a complete dimer covering at occupied sites n_j . The holes, $|\{h_{m_j}\}\rangle_i =$

$\{|2\rangle_{m_j}\}_i$, are at sites m_j , such that $\sum_{j=1}^k 2n_j + \sum_{j=2k+1}^{2N} m_j = 2N$. $r_i = 1, \forall i$. We note that the holes in the lattice are equally distributed between sublattices A and B to necessitate complete dimer coverings but can migrate across all the $2N$ lattice points. See the Appendix for further description.

Characterization of genuine multipartite entanglement.—We use the generalized geometric measure to investigate genuine multipartite entanglement in superconducting GS of the t - J ladder Hamiltonian, under finite doping. The composite hole-spin state can be well-described through a joint three-level system or a qutrit at each site, with the basis $\{|0\rangle_i, |1\rangle_i, |2\rangle_i\}$, and a ladder of length N can be described as a $2N$ -qutrit system [50]. For moderate-sized t - J ladders, the Hamiltonian in Eq. (1) can be exactly diagonalized, by invoking the symmetry properties of the system [51]. Note that $n_{el} = 0$ and 1, correspond respectively to completely vacant and occupied lattices, with the latter being the insulating RVB spin liquid. $x = 1 - n_{el}$ denotes the doping concentration. The GS of the t - J Hamiltonian calculated using exact diagonalization algorithm may lead to degenerate ground state for certain parameters values. To overcome the degeneracy, a finite interaction is introduced in the z -direction of the Heisenberg part of the Hamiltonian, making it an XXZ model. We then estimate \mathcal{G} for upto 14 qutrits.

As shown in the Ref. [38], in the t - J ladder model, the superconducting phase occurs when $J/t \approx 0.6$ with high values of n_{el} . Hence we fix $J/t = 0.66$. The behavior of genuine multisite entanglement in the GS of the t - J ladder, with periodic boundary condition, and upon varying n_{el} , is presented in Fig. 1 for different system sizes. We observe that at $n_{el} = 0$, \mathcal{G} vanishes as expected since it corresponds to a product state, containing only holes. The maximum \mathcal{G} is achieved at a critical density, $n_c = n_{el} \approx 0.65$, which is consistent with doping concentrations at which the superconducting phase occurs in t - J ladders [38]. In the region where $n_{el} < n_c$, \mathcal{G} scales linearly with n_{el} , independent of J/t . This is due to the fact that \mathcal{G} is obtained from the 1:rest bipartition, where the single-site density matrix is diagonal in the computational basis, with elements $[1 - n_{el}, n_{el}/2, n_{el}/2]$. When $1 \geq n_{el} \geq n_c$, the \mathcal{G} is a function of both n_{el} and J/t . Based on the results, one can hypothesize that the trend of \mathcal{G} can detect the superconducting phase boundary, irrespective the size of the ladder.

Let us now investigate the multipartite entanglement of a doped quantum spin ladder, under the RVB ansatz. Since the study of t - J Hamiltonian is limited to numerical simulations and approximate methods, explicit estimation of multipartite entanglement is extremely difficult for large systems. The RVB ansatz for the GS of the t - J model provides a viable alternative to study such quantities. Moreover, our aim is to check whether the RVB GS can effectively capture the trends of multipartite entanglement for the t - J model. It is known that the RVB liquid state with no holes, $|\Psi\rangle_{N,0}$, is rotationally invariant under the unitary $U^{\otimes 2N}$, where U is a local unitary acting on a single qubit [35, 36]. In the composite dimer-hole qutrit space, the doped RVB state, $|\Psi\rangle_{k,N-k}$, is similarly invariant under unitary operations of the form

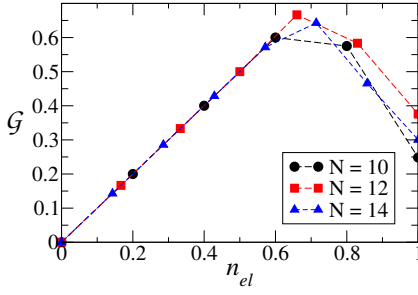


FIG. 1. (Color online). Genuine multisite entanglement in the t - J ladder. Variation of \mathcal{G} with n_{el} for the exact GS of the t - J ladder Hamiltonian, given in Eq. (1), for $N = 10, 12$, and 14 . \mathcal{G} reaches its maximum value at $n_c \approx 0.65$. Here $J/t = 0.66$. All quantities plotted are dimensionless.

$\tilde{U}^{\otimes 2N} = (U \oplus \mathbb{I})^{\otimes 2N}$, where \oplus is the direct sum and \mathbb{I} is the scalar 1. This invariance property of doped RVB ladders is important in investigating its multipartite entanglement as shown in the theorem below.

Theorem: The doped RVB ladder state, $|\Psi\rangle_{k,N-k}$, with $2N$ lattice sites, containing all possible coverings of k ($k \neq 0$) spin dimers interspersed with $2(N-k)$ holes, is always genuinely multipartite entangled for all ladder topologies that are periodic or infinite along the ladder rails.

Proof.— To prove that $|\Psi\rangle_{k,N-k}$ is genuinely multisite entangled, we need to show that the state is entangled across every possible bipartition or alternatively, we have to prove that all reduced density matrices of the system are mixed.

Using the invariance of $|\Psi\rangle_{k,N-k}$ under the action of $\tilde{U}^{\otimes 2N}$, one can show that all p -qutrit reduced systems, $\rho^{(p)} = \text{Tr}_{\bar{p}}[|\Psi\rangle\langle\Psi|_{k,N-k}]$, obtained by tracing over all but p (\bar{p}) sites, is always invariant under $\tilde{U}^{\otimes p}$. Hence, a single qutrit reduced state must have the form, $\rho^{(1)} = p|2\rangle\langle 2| + (1-p)/2 \mathbb{I}_2$, where $\mathbb{I}_2 = |0\rangle\langle 0| + |1\rangle\langle 1|$ and p is fixed by the number of holes in the system. The relation shows that $\rho^{(1)}$ is always mixed for $p \neq 1$. Since all $\rho^{(1)}$ are equivalent, the condition $p = 1$ is satisfied *iff* all $2N$ sites contain holes. Similarly, the two-party reduced state has the form, $\rho^{(2)} = p_1|22\rangle\langle 22| + p_2/9 \mathbb{I}_9 + p_3 W_2(q)$, where \mathbb{I}_9 is the identity matrix on the $\mathbb{C}^3 \otimes \mathbb{C}^3$ and $W_2(q) = q|\psi^-\rangle\langle\psi^-| + (1-q)\mathbb{I}_4/4$ is the Werner state with \mathbb{I}_4 being the identity operator on the 4-dimensional space [52] defined in the projected two-qubit spin basis. Now, $\rho^{(2)}$ is pure when $p_1 = p_2 = 0$ and $q = 1$. Which implies that it is pure *iff* the entire lattice is either filled with holes or is a single dimer covering, and these options are disallowed by the premise. Therefore, $\rho^{(1)}$ and $\rho^{(2)}$ are always mixed and $|\Psi\rangle_{k,N-k}$ is always entangled across these bipartitions.

However, we want to show that all possible bipartitions, irrespective of the number of sites, are always mixed. To prove this let us assume that an arbitrary p -site density matrix ($\rho^{(p)}$) is pure, which implies that $|\Psi\rangle_{k,N-k}$ is separable along that p : $2N-p$. Let $p = p_1 + j$, where $j=1$ or 2 such that $|j| < |p_1|$ ($|\cdot|$ is the cardinality of the argument). For the periodic or infinite ladder, one can always find another

equivalent pure density matrix, $\rho^{(q)}$, such that $q = q_1 + j$ and $|p| = |q|$, where j -sites overlap. By our initial assumption, both $\rho^{(p)}$ and $\rho^{(q)}$ are pure. Using the strong subadditivity of von Neumann entropy $S = -\text{tr}(\sigma \log_2 \sigma)$ [53], we obtain $S(\rho^{(p_1)}) + S(\rho^{(q_1)}) \leq S(\rho^{(p_1+j)}) + S(\rho^{(q_1+j)})$. Now $S(\rho^{(p_1+j)}) = S(\rho^{(q_1+j)}) = 0$, since $\rho^{(p)}$ and $\rho^{(q)}$ are pure. Since $S \geq 0$, we have $S(\rho^{(p_1)}) = S(\rho^{(q_1)}) = 0$, and therefore $S(\rho^{(j)}) = 0$ implying $\rho^{(j)}$ is pure which is not true since all $\rho^{(1)}$ and $\rho^{(2)}$ are mixed under finite doping. Hence, we have a contradiction. Therefore, all reduced density matrices, $\rho^{(p)}$ are mixed and all p : $2N-p$ are entangled.

We note that the above proof does not include the p : $2N-p$ bipartitions where no equivalent $\rho^{(q)}$ with overlap is feasible, such as the bipartition between the two legs of the ladder. However, in such cases, the theorem can be proved using a different argument. We assume that the legs, L_i and L'_i of $|\Psi\rangle_{k,N-k}$ are pure and thus the entire state is separable along that N : N . For the above condition to be satisfied, all reduced states along the rungs, $\rho_{(L_k, L'_k)}^{(2)}$, $\forall k$, must be separable. However, as can be shown by using recursive method, described later in this paper, such nearest-neighbor $\rho^{(2)}$ states are always entangled. Hence, the doped RVB state is genuinely multipartite entangled. ■

Although the above theorem proves that the doped RVB state is always genuinely multipartite entangled, analysis of \mathcal{G} requires its computation for large systems. We propose an analytical method to recursively build the doped RVB state from smaller systems and subsequently obtain its relevant reduced density matrices which is necessary to study multipartite entanglement.

Recursive method to generate the doped RVB state.—To overcome the complexity [54] in analyzing large doped RVB ladders, we recursively [34, 55] construct the state $|\psi\rangle_{k,N-k}$, defined in Eq. (2). Let us begin with an open $2N$ site ladder lattice with all vacant sites (holes), which is successively filled with dimers. We use the notation, $|N-k, k\rangle$ to denote the N -rung ladder, $|\psi\rangle_{k,N-k}$, containing $2k$ spins filled with dimers and $2(N-k)$ holes. The state $|N-k, k\rangle$ is achieved by successively filling k dimers in the $|N, 0\rangle$ state, i.e., $|N, 0\rangle \xrightarrow{k} |N-k, k\rangle$. For an analytical method which allows us to build the superpositions in an arbitrary $|N-k, k\rangle$, we propose the generator: $|N-k, k\rangle = \mathcal{U}^{\otimes k'=1} |N-k+1, k-1\rangle + |N-k-1, 0\rangle |\chi_{k+1}\rangle + |N-k-2, 0\rangle |\chi_{k+1}\rangle |1, 0\rangle$, where $\mathcal{U}^{\otimes k'}$ is the operator to add k' dimers.

The methodology to derive the recursion relation and the description of $|\chi_{k+1}\rangle$ is given in the Appendix. In order to calculate the \mathcal{G} of the doped RVB state, we required to derive expressions for the reduced density matrices, using the generator. Numerical studies for a moderate N , suggest that obtaining the reduced state of a square block of 4 sites for large ladders, which is symmetric for the ladder, is sufficient for the computation of \mathcal{G} . Hence, we use the recursion method to obtain the 4-site reduced state (ρ_{red}) at rungs $m-1$ and m . Let us consider the cases for open and periodic ladders separately.

a) *Open ladder:* The primary method to build the recursive

relations is to divide the lattice into blocks and junctions. The advantage lies in the fact that these blocks do not overlap, and hence can be independently traced to obtain ρ_{red} needed to

calculate the \mathcal{G} . Hence, from the non-periodic ladder state, $|N - k, k\rangle$, by tracing all sites apart from rungs $m - 1$ and m , we get the reduced state, $\rho_{red}^{\mathcal{NP}}$, of 4-sites, is recursively generated via,

$$\begin{aligned} \rho_{red}^{\mathcal{NP}} = & \sum_{i=0}^2 \mathcal{Z}_{(k-i)}^{(S-1+i)} |2-i, i\rangle \langle 2-i, i| + \sum_{k_1=2}^{k+1} \mathcal{Z}_{(k-k_1+1)}^{(S-1)} \text{tr}(|\chi_{k_1}\rangle \langle \chi_{k_1}|) |1'\rangle \langle 1'| + \sum_{k_2=2}^k \mathcal{Z}_{(k-k_2)}^{(S)} \text{tr}(|\chi_{k_2}\rangle \langle \chi_{k_2}|) |1\rangle \langle 1| \\ & + \sum_{i=0}^1 \mathcal{Z}_{(k-2-i)}^{(S+i)} \text{tr}(|\bar{2}\rangle \langle \bar{2}|) |1-i, i\rangle \langle 1-i, i| + \sum_{k_3=3}^{k+1} \mathcal{Z}_{(k-k_3+1)}^{(S)} (\text{tr}(|\chi_{k_3}\rangle \langle \chi_{k_3}|)) + \sum_{k_4=2}^k \mathcal{Z}_{(k-k_4)}^{(S)} (\text{tr}(|\chi_{k_4+1}\rangle \langle \chi_{k_4}|) |1\rangle \langle 1|) \\ & + \text{h.c.}) + \sum_{i=0, j=0}^{i=1, j=k-2-i} \mathcal{Z}_{(k-2-i-j)}^{(S+i)} (1/2)^{j+1} (|1\rangle |1-j, j\rangle \langle 1-j, j+1| + \text{h.c.}), \text{ where } S = N - k - 1, \text{ and} \end{aligned} \quad (3)$$

$\mathcal{Z}_k^{N-k} = \langle N - k, k | N - k, k \rangle$, and $|\bar{2}\rangle = |0, 2\rangle - |0, 1\rangle |1, 0\rangle$.
b) *Periodic ladder*: Incorporation of periodic boundary condition, $N + 1 \equiv N$, leads to additional terms in the state $|N - k, k\rangle$. Consequently, we find that the number of terms in the expression of the recursively generated reduced den-

sity matrix, $\rho_{red}^{\mathcal{P}}$, increases, due to overlap of different states. These extra terms in $\rho_{red}^{\mathcal{P}}$ can be redeemed by analyzing two separate situations, say \mathcal{P}_1 and \mathcal{P}_2 as described in Appendix. The type \mathcal{P}_1 leads to reduced states given by Eq. (4), while for $N - k = 1$ and $= 2$, \mathcal{P}_2 leads to Eqs. (5) and (6), respectively.

$$\begin{aligned} \rho_{red}^{\mathcal{P}_1} = & \text{tr}(|\zeta\rangle \langle \zeta|) + \frac{1}{2} \sum_{i=0, j=0}^{i=1, j=k-2-i} \mathcal{Z}_{(k-2-i-j)}^{(S+i)} \left(\frac{1}{2}\right)^j |1-i, i\rangle |1\rangle \langle i-1, i+1| + \frac{1}{2} \sum_{j=0}^{j=k-4} \mathcal{Z}_{(k-4-j)}^{(S+1)} \left(\frac{1}{2}\right)^j \text{tr}(|\bar{2}\rangle \langle \bar{2}|) |1\rangle \langle 1| \\ & + \left(\frac{1}{2}\right)^j \sum_{k_6=2, j=0}^{k_6=k-1, j=k-k_6-1} \mathcal{Z}_{(k-k_6-1-j)}^{(S)} \left(\frac{1}{2}\right)^j \text{tr}(|\chi_{k_6}\rangle \langle \chi_{k_6}| |1\rangle \langle 1| + |\chi_{k_6}\rangle |1\rangle \langle \chi_{k_6+1}|) + \frac{1}{2} \sum_{i=0, j=0}^{j=k-4-i} \mathcal{Z}_{(k-4-(i+j))}^{(S+1)} \left(\frac{1}{2}\right)^{i+j} \\ & \times \text{tr}(|\bar{2}\rangle |1\rangle \langle 1| \langle \bar{2}|) + \frac{1}{2} \sum_{i=0, j=0, l=0}^{i=1, j=k-3-i, l=k-3-(i+j)} \mathcal{Z}_{(k-3-(i+j+l))}^{(S+i)} \left(\frac{1}{2}\right)^{j+l} \text{tr}(|1\rangle |1-i, i\rangle |1\rangle \langle \bar{2}| \langle 1-i, i|), \end{aligned} \quad (4)$$

$$\rho_{red}^{\mathcal{P}_2} = |\gamma_1\rangle \langle \gamma_1| + |\gamma_2\rangle \langle \gamma_2| + \left(\frac{1}{2}\right)^{k-3} (|\gamma_1\rangle \langle \gamma_2| + |\gamma_2\rangle \langle \gamma_1|) + [(|\gamma_1\rangle + |\gamma_2\rangle)(\mathcal{D}_{k-2} \langle 1 | \bar{2} \rangle \langle 1' | + \mathcal{D}_{k-1} \langle H |) + \text{h.c.}] (-1)^{k+1/2}, \quad (5)$$

$$\rho_{red}^{\mathcal{P}_2} = (|\xi\rangle \langle \xi| + |\xi\rangle \langle \chi_2 | \langle 1' |) (-1)^{k/2-1} \mathcal{D}_{k-1}, \text{ where, in Eq. (4), } S = N - k - 1. \quad (6)$$

Here the term $|\xi\rangle$, $|\gamma_{1(2)}\rangle$, and $|\zeta\rangle$ are described in the Appendix and \mathcal{D}_k can recursively be generated using $\mathcal{D}_x = \mathcal{D}_{x-1} + 2\mathcal{D}_{x-2}$ with the initial condition $\mathcal{D}_0 = \mathcal{D}_1 = 1$. Now if $N - k = 1$, periodic states corresponding to the two types, \mathcal{P}_1 and \mathcal{P}_2 , would overlap with each other and lead to the following additional terms in the expression of the total reduced density matrix of 4-sites given by, $\rho_{red}^{\mathcal{P}_{12}} = 1/2^{(k-3)} (-1)^{(k+1)/2} (|\gamma\rangle \langle \gamma_1| + \langle \gamma_2| + \text{h.c.}) \mathcal{D}_{k-3}$, where $|\gamma\rangle = |\bar{2}\rangle_{1,N} |N - k - 2, k - 2\rangle_{2,N-1}$. Hence considering all possible periodic boundary terms, the expression of the reduced density matrix for the system is given by $\rho_{red}^{\mathcal{P}} = \rho_{red}^{\mathcal{NP}} + \rho_{red}^{\mathcal{P}_1}$

+ $\rho_{red}^{\mathcal{P}_2} + \rho_{red}^{\mathcal{P}_{12}}$. Fig. 2 shows the \mathcal{G} of a periodic doped RVB state calculated using the recursion method for upto 200 lattice sites. We observe that the maximum \mathcal{G} occurs at $n_{el} = n_c \approx 0.56$, which corresponds to the superconducting phase of the t - J model at $J/t = 0.66$. A detailed description of the recursion method is provided in the Appendix.

Discussion.—In this work, we investigated the characteristics of genuine multipartite entanglement of the superconducting phase in the ground state of the t - J ladder Hamiltonian under moderately high doping concentration ($x \approx 0.4$). Different properties like classical correlation, spin gap, energy spec-

tra have been predicted by various theoretical studies based on mean-field approximations and numerical methods. In this paper, we adopt two techniques for studying multisite entanglement of this model. Firstly, we use exact diagonalization, for upto 14 sites and observe that the GS of the Hamiltonian is genuinely multipartite entangled, with maximum entanglement occurring at the superconducting phase boundary, where the electron density $n_{el} \approx 0.65$. Secondly, our results on the

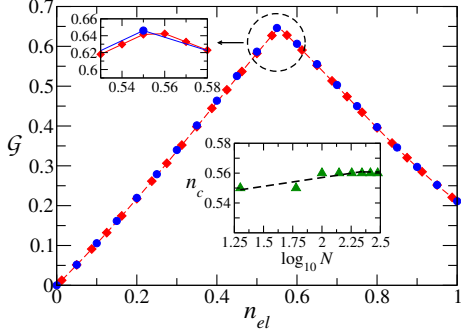


FIG. 2. (Color online.) Genuine multisite entanglement in doped RVB ladder. Variation of \mathcal{G} with n_{el} in doped RVB ladder states, for $2N = 40$ (blue circles) and 200 (red diamonds) lattice sites. The top inset magnifies the encircled region in the plot. The bottom inset shows the scaling of n_c with the $\log_{10} N$. The inset shows that as N increases (plotted up to 300 sites), n_c converges to 0.56 . This is to be compared to the result for the moderate-sized systems described by the t - J model in the superconducting regime, in Fig 1.

t - J Hamiltonian is supported by considering the RVB ground states, under finite doping of the ladder. We prove that the doped RVB ladder is always genuinely multipartite entangled and to overcome the limitations of exact diagonalization, we introduce a recursion method to generate the doped RVB state and to compute its reduced density matrices. By using the iterative method, we show that we can compute the genuinely multipartite entanglement measure of the doped RVB ladders, for upto 300 sites, and show that its maximum value in the electron density in to the superconducting phase of the t - J ladder. This is in contrast to the results known for small 2D square RVB lattices, where the maximum geometric entanglement is observed for small doping concentrations [37].

Our results show that the superconducting states of the doped quantum spin ladders are maximally genuine multipartite entangled, at relatively high doping concentration, as described by the phase diagram of the t - J Hamiltonian [38]. In this regime, one can expect that the strong correlation in the superconducting currents should emanate from robust multipartite entanglement in the doped system although we note that there is no universal agreement on the phase separation or ground state correlations associated with high- T_c superconductors. We conclude about such a high multipartite entanglement in a superconducting phase of a t - J model by using exact diagonalization and by using doped RVB ansatz. For numerical exact diagonalization we choose Lanczos algorithm while to compute doped RVB states, we developed an analytical recursion method capable of calculating any physical

quantities of a state with a large number of sites. We believe that our results are an addition to the broader understanding of the nature of quantum correlations in the states commonly associated with exotic superconductivity in strongly correlated system.

APPENDIX

I. The doped quantum spin ladder

In our work, the quantum spin ladder with $2N$ lattice sites is described using a periodic *bipartite lattice*, where the ladder is divided into two sublattices A and B , such that all nearest-neighbor sites corresponding to a site in sublattice, A belong to sublattice B and vice-versa. This implies that all nearest-neighbor interactions in the Hamiltonian occur between sites belonging to different sublattices. A bipartite lattice, in a ladder configuration, is shown in Fig. 3.

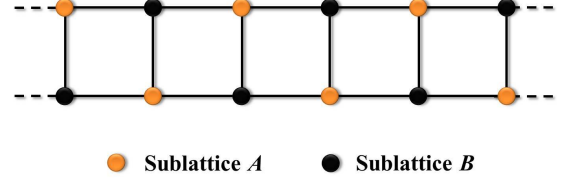


FIG. 3. Schematic diagram of a bipartite ladder lattice, with sublattices A and B . In the figure, the periodicity of the lattice is shown by dotted lines at the two ends.

The spin ladder is doped by introducing vacant sites or “holes” in the lattice, as shown in Fig. 4. The composite hole-spin state in a doped quantum spin ladder can be well described through a joint three-level or a qutrit system, as mentioned in the main text. A single spin is represented by the two-level basis $\{|\uparrow\rangle_\sigma, |\downarrow\rangle_\sigma\}$, with each lattice site described by an additional occupancy vector $\{|0\rangle_\Omega, |1\rangle_\Omega\}$, which refers to the vacant and occupied site, respectively. Hence, a hole can be ideally considered as the vacuum state $|0\rangle_\Omega$. The system, at site i , can exist in three possible states: $|\uparrow\rangle_{\sigma,i}|1\rangle_{\Omega,i}$, $|\downarrow\rangle_{\sigma,i}|1\rangle_{\Omega,i}$, and $|0\rangle_{\Omega,i}$. Hence, the superconductor can be described using a three-level system or a qutrit at each site, with the basis $\{|0\rangle_i, |1\rangle_i, |2\rangle_i\}$, and a ladder of length N can be described as a $2N$ qutrit system.

As mentioned in the text, for moderate sized t - J ladders, at half-filling, the Hamiltonian in Eq.(1) can be exactly diagonalized, provided certain properties of the system are invoked [50]. For example, the spin number Hamiltonian, $\hat{N} = \sum_i (|0\rangle\langle 0| + |1\rangle\langle 1|)_i$, and the total spin along the z -axis, $\hat{S}^z = \sum_i S_i^z$ commute with the Hamiltonian, \mathcal{H} . Hence, the Hamiltonian can be block-diagonalized in the $(\mathbb{C}^3)^{\otimes 2N}$ Hilbert space basis for different total spin \hat{S}^z and electron density $n_{el} = \langle \hat{N} \rangle / 2N$. For our case, we assume that the spins form an initial insulating phase with $\hat{S}^z = 0$, and with n_{el} varying from 0 to 1. Note that $n_{el} = 0$ and 1, correspond to a completely vacant and occupied lattice, respectively. For

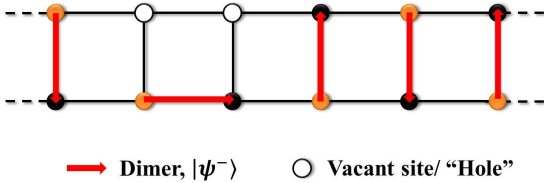
$n_{el} = 1$, the state is an insulating RVB spin liquid. The doping concentration is denoted by $x = 1 - n_{el}$. In our work, we have developed a numerical algorithm [51], based on the Lanczos method [56], to exactly solve the composite hole-dimer qutrit system. By dividing the Hilbert space in different subspaces, according to the hole concentration x and total \hat{S}^z , exact ground state of the t - J Hamiltonian can be obtained for upto 14 qutrits, with even number of holes. The algorithm is implemented using codes written in MATLAB and Fortran90.

Beyond exact diagonalization, the ground states of the t - J Hamiltonian can be investigated using the RVB ansatz. Various theoretical studies show that the ground states of the t - J Hamiltonian has a spin liquid ground state with a finite spin gap in the excitation spectra, thus supporting the RVB ansatz. Let us consider the doped RVB state containing $2N$ lattice sites, on a ladder configuration, with $2k$ spin-1/2 particles and $2(N - k)$ holes or vacant lattice sites. To cover a ladder with dimers consistently, one represents the ladder using a *bipartite lattice*, consisting of sublattices A and B . The doped RVB state consists of equal-weight superposition of all possible coverings of k NN dimers with $2(N - k)$ holes arranged in such a way as to allow a complete covering of the two-legged ladder as shown in Figs. 4-5.

As mentioned in the main text, the wavefunction of the doped RVB state, for a fixed electron density, $n_{el} = k/N$, can be written as

$$|\psi\rangle_{k,N-k} = \sum_i r_i |(a_{n_1} b_{n_1})(a_{n_2} b_{n_2}) \cdots (a_{n_k} b_{n_k})\rangle_i \otimes |h_{m_{2k+1}} h_{m_{2k+2}} \cdots h_{m_{2N}}\rangle_i, \quad (7)$$

where $|(a_{n_j} b_{n_j})\rangle$ is a dimer, with $a_j \in A$ and $b_j \in B$. $\{|(a_{n_j} b_{n_j})\rangle\}_i$ represents a complete dimer covering at occupied sites n_j , with the holes, $\{|h_{m_j}\rangle\}_i$, at sites m_j , such that $\sum_{j=1}^k 2n_j + \sum_{j=2k+1}^{2N} m_j = 2N$. $p_i = 1, \forall i$. We note that the holes in the lattice are equally distributed between sublattices A and B to necessitate complete dimer coverings but can migrate across all the $2N$ lattice points.



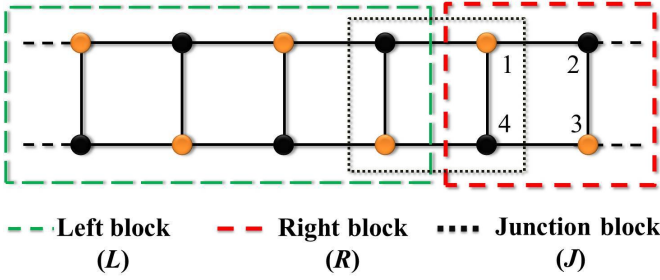


FIG. 6. Schematic diagram of the blocks L , R , and J in the spin lattice. To compute \mathcal{G} , we obtain the reduced density matrix (ρ_{red}) corresponding to the sites 1-4 in the R block. The rest of the lattice is traced out. Numerical studies show that the reduced state ρ_{red} is sufficient to compute \mathcal{G} in doped RVB states.

An important aim of the recursion method to generate the doped RVB state $|N - k, k\rangle$ is to successfully obtain the reduced state ρ_{red} . To facilitate our calculations, we divide the $2N$ ladder lattice into specific regions that can be filled with dimers. We start by splitting the initial state $|N, 0\rangle$ into two regions, denoted by left (L) and right (R) block, such that

$$|N, 0\rangle = |N - 2, 0\rangle_L \otimes |2, 0\rangle_R. \quad (9)$$

This is explicitly shown in Fig. 6. We note that the block R is the region which contain the desired reduced density matrix (ρ_{red}), obtained by tracing out the state on the rest of the lattice sites. An important region is the junction (J) block between L and R blocks, which is shown in Fig. 6 using a black-dotted square. The blocks, excluding overlapping region, can be written as:

$$|N - 3, 0\rangle_{L'} \otimes |2, 0\rangle_J \otimes |1, 0\rangle_{R'},$$

where L' (R') implies the region $L - L \cap J$ ($R - R \cap J$).

Now starting from an initial configuration $|N, 0\rangle$, our aim is to reach the final state $|N - k, k\rangle$ by systematically introducing k numbers of dimers in the different blocks of the lattice. The first dimer is introduced in the initial hole configuration though the following possible ways:

1. *Update the left block:* In this step, a dimer is introduced into the L block and the updated state is

$$|N - 2, 0\rangle_L |2, 0\rangle_R \xrightarrow{k=1} |N - 3, 1\rangle_L |2, 0\rangle_R. \quad (10)$$

2. *Update the right block:* Similarly, in the next step, a dimer is injected into the R block. The updated state looks like

$$|N - 2, 0\rangle_L |2, 0\rangle_R \xrightarrow{k=1} |N - 2, 0\rangle_L |1, 1\rangle_R. \quad (11)$$

3. *Update of the junction block:* In this step a dimer is introduced in the junction of the L and R blocks, i.e., the J block. The updated state turns out to be

$$|N - 2, 0\rangle_L |2, 0\rangle_R \xrightarrow{k=1} |N - 1, 0\rangle |\chi_2\rangle |1, 0\rangle, \quad (12)$$

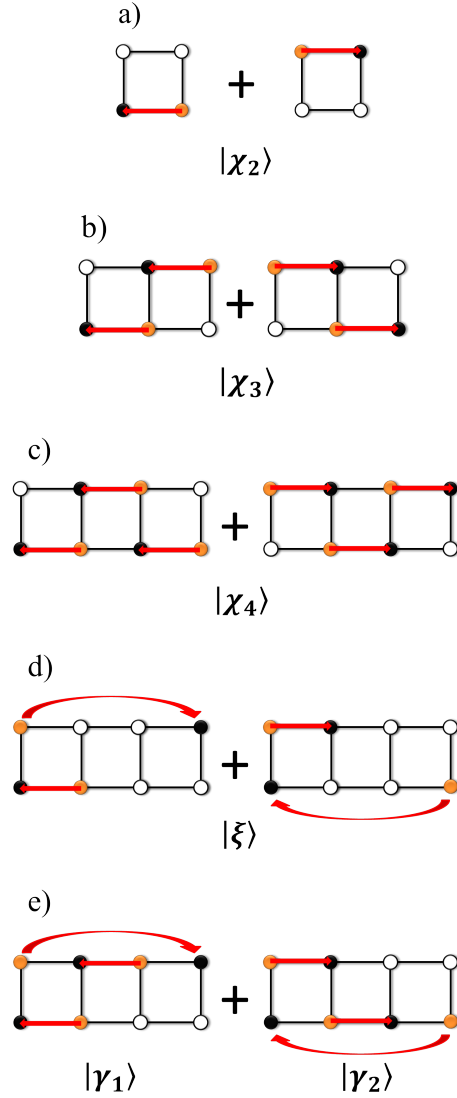


FIG. 7. Schematic diagram of the states: a) $|\chi_2\rangle$, b) $|\chi_3\rangle$, c) $|\chi_3\rangle$, and the periodic terms: d) $|\xi\rangle$, and e) $|\gamma_1\rangle$ and $|\gamma_2\rangle$, used in the recursion relations.

where the state $|\chi_2\rangle$ is depicted in Fig. 7(a). Now combining the above three steps, the final state after introduction of a single dimer in the lattice is given by

$$\begin{aligned} |N, 0\rangle &\xrightarrow{k=1} |N - 1, 1\rangle \\ &\equiv |N - 3, 1\rangle_L |2, 0\rangle_R + |N - 2, 0\rangle_L |1, 1\rangle_R \\ &+ |N - 1, 0\rangle |\chi_2\rangle |1, 1\rangle. \end{aligned} \quad (13)$$

For example, consider the initial state $|4, 0\rangle$ in Eq. (8). We have, $|4, 0\rangle = |2, 0\rangle_L |2, 0\rangle_R$. Then the state, after introduction of one dimer, would be (see Fig. 8 for an illustration of the three update paths)

$$\begin{aligned} |4, 0\rangle &\xrightarrow{k=1} |3, 1\rangle = |1, 1\rangle |2, 0\rangle + |2, 0\rangle |1, 1\rangle \\ &+ |1, 0\rangle |\chi_2\rangle |1, 0\rangle, \end{aligned} \quad (14)$$

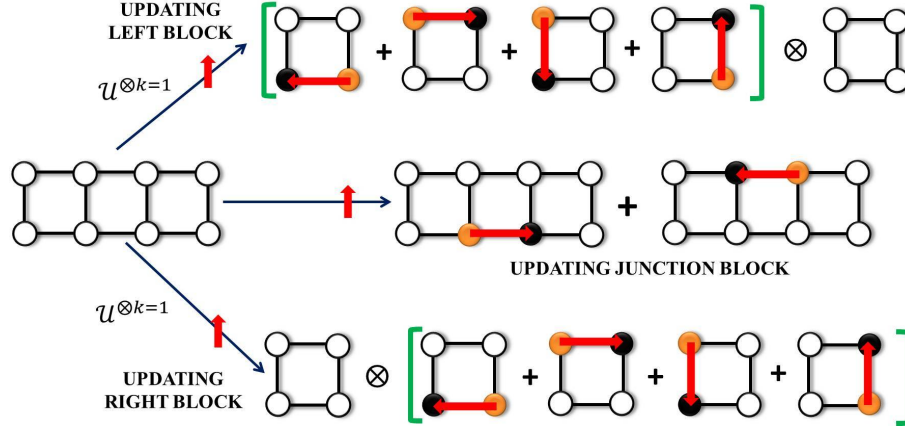


FIG. 8. Schematic diagram of the scheme to build a doped-RVB state from a lattice filled with holes, for an 8 site RVB ladder, as given by the process: $|4, 0\rangle \xrightarrow{k=1} |3, 1\rangle$, described in Eq. (8).

where the first two terms are the contributions from the blocks L and R , and the third term comes from the update of the junction, J .

Now after completion of the first step, we need to introduce one more dimer into the present configuration in order to continue the iteration process. It can be done following a path similar to the one described above, i.e., a direct update of the L and R blocks, which is basically updating all the terms of the state by introducing dimers into the left and right blocks, and an update, which consists of injecting a dimer at the junction block. The above scheme can be repeated k times so that the final state contains k dimers and $2(N - k)$ holes in the lattice. In general, by updating the L , J , and R blocks, with $k' = 1$ singlets, we obtain the recursive generator to obtain the RVB state, which can be written as

$$|N - k, k\rangle = \mathcal{U}^{\otimes k'=1} |N - k + 1, k - 1\rangle + |N - k - 1, 0\rangle \times |\chi_{k+1}\rangle + |N - k - 2, 0\rangle |\chi_{k+1}\rangle |1, 0\rangle, \quad (15)$$

where $\mathcal{U}^{\otimes k'}$ is the direct update operator to inject k dimers in the L and R blocks of the state, $|N - k + 1, k - 1\rangle$. Subsequently, the second and the third terms in Eq. (15) correspond to the indirect update of the J block. For example, the first two terms in Eq. (14), $|1, 1\rangle |2, 0\rangle$ and $|2, 0\rangle |1, 1\rangle$, is generated from the direct update of the state $|4, 0\rangle$ and the third term $|1, 0\rangle |\chi_2\rangle |1, 0\rangle$ emerges from the indirect update of the junction sites. Note that, there may arise similar terms due to the update process of the L , R , and the J block. In those cases we need to carefully include such terms only once in the recursion, so that overcounting of the terms can be avoided. In Eq. (15), we note that the term $|\chi_{k+1}\rangle$ can be generated recursively from $|\chi_k\rangle$ by introducing an additional rung to the left and assigning a dimer along the horizontal direction, as demonstrated in Fig. 7, for $|\chi_2\rangle$, $|\chi_3\rangle$ and $|\chi_4\rangle$.

Formation of reduced density matrix: The main advantage in formulating such a recursion relation for the entire state can be seen when one needs to obtain the reduce density ma-

trix, ρ_{red} . This is because the terms which correspond to the blocks R and L are mutually orthogonal to those belong to the junction block J . As a result, in the expression for ρ_{red} , one would never get any contribution from the terms that emanate from $|\bullet\rangle_{L(R)} \langle \bullet|_J$. Now if one starts from the L and R blocks coverings and traces out all but the sites of last two rungs (sites (1-4) in Fig. 6), then there would be the following three possibilities,

- i) The reduced block contains holes only.
- ii) The reduced block contains one singlet and one pair of hole.
- iii) The reduced block contains singlet coverings only.

The first term in Eq. (3), in the main text,

$$\sum_{i=0}^2 \mathcal{Z}_{(k-i)}^{(\mathcal{S}-1+i)} |(2-i), (i)\rangle \langle (2-i), (i)|$$

basically corresponds to the above possibilities. As an example, consider an initial eight-site doped RVB state which includes only one singlet and 3 hole-pairs. The contribution from the L block and R block would lead to the following terms in the expression of the doped RVB state, $|1, 1\rangle_L \otimes |2, 0\rangle_R + |2, 0\rangle_L \otimes |1, 1\rangle_R$. Therefore, the reduced state would contain following terms, $a_1 |2, 0\rangle \langle 2, 0| + a_2 |1, 1\rangle \langle 1, 1|$, where $a_1 = \mathcal{Z}_1^1$, and $a_2 = \mathcal{Z}_0^2$ is obtained from Eq. (3).

Subsequently, the junction J would generate additional terms in the expression of the reduced state. As an example, first consider terms which has only one singlet at the junction block (see Fig. 7). Mathematically, those can be expressed as $|\bullet\rangle \otimes |\chi_k\rangle \otimes |\bullet\rangle$, where $|\chi_2\rangle$ and $|\chi_3\rangle$ are depicted in Fig. 7. Now the contributions from the overlap of those terms are given by second, third, and fourth terms in Eq. (3). Considering, once more, the previous example of an eight-site doped RVB state containing only one singlet, we can write the contributing term from the junction as $|1, 0\rangle \otimes |\chi_2\rangle \otimes |1, 0\rangle$. Hence after tracing out all but the sites those are at the last two-rungs,

we get

$$\rho_{red}^{\mathcal{NP}} = a_1 |2, 0\rangle\langle 2, 0| + a_2 |1, 1\rangle\langle 1, 1| + a_3 \text{tr} |\chi_2\rangle\langle \chi_2| \otimes |1, 0\rangle\langle 1, 0|, \quad (16)$$

where $a_3 = \mathcal{Z}_0^1$ is again evaluated using Eq. (3).

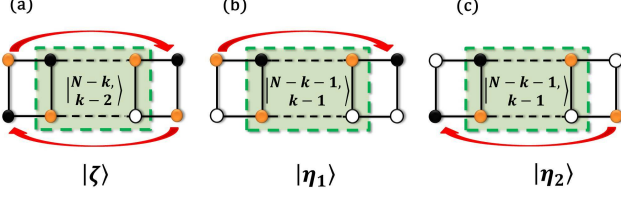


FIG. 9. Schematic diagram of the blocks L , R , and J in the spin lattice with periodic boundary condition.

Additionally, there may be terms which would contain two horizontal singlets at the junctions such as $|\bullet\rangle \otimes |\bar{2}\rangle \otimes |\bullet\rangle$. Those would certainly have non-zero overlap with the L and R block terms. The fifth and sixth terms in the Eq. (3) correspond to contribution from these terms. As an example, instead of inserting one singlet if we now introduce two singlets in the eight-site doped RVB state i.e. $|2, 2\rangle$, we would have terms in the doped RVB state such as $|1, 0\rangle \otimes |\bar{2}\rangle \otimes |1, 0\rangle$. Hence the reduced density matrix would have following terms,

$$a_4 \text{tr} |\bar{2}\rangle\langle \bar{2}| \otimes |1, 0\rangle\langle 1, 0| + a_5/2 |0, 1\rangle\langle 1, 0| \langle H|,$$

where a_4 and a_5 are given by \mathcal{Z}_0^1 which can be obtained from Eq. (3), for $N = 4$ and $k = 2$.

Now in case of periodic boundary conditions, some contribution would arise due to the presence of following situations:

I – the end sites of both the legs share a singlet (see Fig. 9(a))

II – the end sites of only one of the leg share a singlet and the end site of the other leg contains holes (see Figs. 9(b) and (c))

Therefore, in the expression of the reduced density matrix, there would be additional terms due to the overlap of the states in I with itself, and the L and R blocks ($\rho_{red}^{\mathcal{P}_1}$) and similarly, the overlap of states in II with itself, and L and R blocks ($\rho_{red}^{\mathcal{P}_2}$). Moreover, some additional terms may appear due to the overlap between the blocks I–II ($\rho_{red}^{\mathcal{P}_{12}}$). These terms will accordingly contribute to the final reduced state, ρ_{red} , as shown in Eqs. (4-6) of the main text.

III. Genuine multiparty entanglement measure (GGM)

The genuine multisite entanglement measure \mathcal{G} , of an N -party pure quantum state $|\phi\rangle$ is a computable measure. The GGM of an N -party quantum state is basically the optimized fidelity distance of the state from the set of all states that are

not genuinely multiparty entangled. In particular, the GGM $\mathcal{G}(|\phi\rangle)$ can be evaluated as

$$\mathcal{G}(|\phi\rangle) = 1 - \lambda_{\max}^2(|\xi_n\rangle)$$

where $\lambda_{\max} = \max \langle \xi_n | \phi \rangle$, $|\xi_n\rangle$ is an N -party non-genuinely multisite entangled quantum state and the maximization is performed over the set of all such states. For pure quantum states GGM can be effectively computed using the straightforward relation

$$\mathcal{G}(|\xi\rangle) = 1 - \max \{ \lambda_{A:B}^2 | A \cup B = A_1, \dots, A_N, A \cap B = \phi \},$$

where $\lambda_{A:B}$ is the maximum Schmidt coefficient in all possible bipartition split of $A : B$ of the given state $|\phi\rangle$.

-
- [1] J. G. Bednorz, and K. A. Müller, 1986, *Possible high T_c superconductivity in the Ba-La-Cu-O system*, Z. Phys. B **64**, 189 (1986).
 - [2] P. W. Anderson, *The Theory of Superconductivity in the High- T_c Cuprate Superconductors*, Princeton University Press, Princeton (1997); P. Anderson, P. Lee, M. Randeria, T. M. Rice, N. Trivedi, F. Zhang, *The physics behind high-temperature superconducting cuprates: the 'plain vanilla' version of RVB*, J. Phys. Condens. Matter **16**, 755 (2004).
 - [3] E. Dagotto, *Correlated electrons in high-temperature superconductors*, Rev. Mod. Phys. **66**, 763 (1994).
 - [4] P. A. Lee, N. Nagaosa, and X.-G. Wen, *Doping a Mott insulator: Physics of high-temperature superconductivity*, Rev. Mod. Phys. **78**, 17 (2006).
 - [5] B. Keimer, S. A. Kivelson, M. R. Norman, S. Uchida, and J. Zaanen, *From quantum matter to high-temperature superconductivity in copper oxides*, Nature (London) **518**, 179 (2015).
 - [6] Z. J. J. Stekly and E. Gregory, *Applications for high-temperature superconductors*, in *High-Temperature Superconducting Materials Science and Engineering: New Concepts and Technology*, edited by D. Shi, Elsevier Science, Oxford (1995).
 - [7] K. H. Mess, P. Schmüser, and S. Wolff, *Superconducting accelerator magnets*, World Scientific, Singapore (1996); H. Padamsee, T. Hays, J. Knobloch, *RF superconductivity for accelerators*, 2nd ed., Wiley-VCH, New York (2008).
 - [8] D. Koelle, R. Kleiner, F. Ludwig, E. Dantsker, and J. Clarke, *High-transition-temperature superconducting quantum interference devices*, Rev. Mod. Phys. **71**, 631 (1999); M. Chukharkin, A. Kalabukhov, J.F. Schneiderman, F. Öisjöen, O.V. Snigirev, Z. Lai, D. Winkler, *Noise properties of high- T_c superconducting flux transformers fabricated using chemical-mechanical polishing*, Appl. Phys. Lett. **101**, 042602 (2012); E. Y. Cho, M. K. Ma, C. Huynh, K. Pratt, D. N. Paulson, V. N. Glyantsev, R. C. Dynes, and S. A. Cybart, *$YBa_2Cu_3O_{7-\delta}$ superconducting quantum interference devices with metallic to insulating barriers written with a focused helium ion beam*, Appl. Phys. Lett. **106**, 252601 (2015).
 - [9] N. F. Mott., *The Basis of the Electron Theory of Metals, with Special Reference to the Transition Metals*, Proc. Phys. Soc. A **62**, 416 (1949).
 - [10] K. Onnes, *The resistance of pure mercury at helium temperatures*, H. Commun. Phys. Lab. Univ. Leiden No. 120 (1911).
 - [11] J. Bardeen, L. N. Cooper, and J. R. Schrieffer, *Theory of Superconductivity*, Phys. Rev. **108**, 1175 (1957).

- [12] We note that recent studies have observed high temperature superconductivity in conventional superconductors, at critical temperatures above 200K, using hydrogen sulphide under extremely high pressure. See Ref. [13, 14].
- [13] A. P. Drozdov, M. I. Erements, I. A. Troyan, V. Ksenofontov, and S. I. Shylin, *Conventional superconductivity at 203 kelvin at high pressures in the sulfur hydride system*, Nature (London) **525**, 73 (2015).
- [14] N. W. Ashcroft, *Metallic Hydrogen: A High-Temperature Superconductor?* Phys. Rev. Lett. **21**, 1748 (1968); X. J. Zhou et al., *Dichotomy between Nodal and Antinodal Quasiparticles in Underdoped $(\text{La}_{2-x}\text{Sr}_x)\text{CuO}_4$ Superconductors*, Phys. Rev. Lett. **92**, 187001 (2004). V. L. Ginzburg, *Superfluidity and superconductivity in the universe*, J. Stat. Phys. **1**, 3 (1969).
- [15] B. Batlogg, *A critical review of selected experiments in high-T_c superconductivity*, Physica B **169**, 7 (1991); T. Timusk and B. Statt, *The pseudogap in high-temperature superconductors: an experimental survey*, Rep. Prog. Phys. **62**, 61 (1999); A. Damascelli, Z. Hussain, and Z.-X. Shen, *Angle-resolved photoemission studies of the cuprate superconductors*, Rev. Mod. Phys. **75**, 473 (2003).
- [16] A. J. Leggett, *What DO we know about high T_c?*, Nat. Phys. **2**, 134 (2006); A. Mann, *High-temperature superconductivity at 25: Still in suspense*, Nature (London) **475**, 280 (2011).
- [17] P. W. Anderson, *The Resonating Valence Bond State in La_2CuO_4 and Superconductivity*, Science **235**, 1196 (1987).
- [18] C. Gros, *Superconductivity in correlated wave functions*, Phys. Rev. B **38**, 931(R) (1988).
- [19] K. A. Chao, J. Spałek, and A. M. Oleś, *Kinetic exchange interaction in a narrow S-band*, J. Phys. C **10**, L271 (1977); *Canonical perturbation expansion of the Hubbard model*, Phys. Rev. B **18**, 3453 (1978); A. Auerbach, *Interacting Electrons and Quantum Magnetism*, Springer, Berlin, 1998.
- [20] E. Dagotto, J. Riera, and D. Scalapino, *Superconductivity in ladders and coupled planes*, Phys. Rev. B **45**, 5744(R) (1992); S. Gopalan, T. M. Rice, and M. Sigrist, *Spin ladders with spin gaps: A description of a class of cuprates*, Phys. Rev. B **49**, 8901 (1994); T. Barnes and J. Riera, *Susceptibility and excitation spectrum of $(\text{VO})_2\text{P}_2\text{O}_7$ in ladder and dimer-chain models*, Phys. Rev. B **50**, 6817 (1994).
- [21] M. Sigrist, T. M. Rice, and F. C. Zhang, *Superconductivity in a quasi-one-dimensional spin liquid*, Phys. Rev. B **49**, 12058 (1994); R. M. Noack, S. R. White, and D. J. Scalapino, *Correlations in a Two-Chain Hubbard Model*, Phys. Rev. Lett. **73**, 882 (1994); D. V. Khveshchenko and T. M. Rice, *Spin-gap fixed points in the double-chain problem*, Phys. Rev. B **50**, 252 (1994); B. Edegger, V. N. Muthukumar, and C. Gros, *Gutzwiller–RVB theory of high-temperature superconductivity: Results from renormalized mean-field theory and variational Monte Carlo calculations*, Adv. Phys. **927**, 1033 (2007).
- [22] M. Ogata, M. U. Luchini, and T. M. Rice, *Spin gap in a generalized one-dimensional t-J model*, Phys. Rev. B **44**, 12083(R) (1991); M. Imada, *Spin-gap state and superconducting correlations in a one-dimensional dimerized t-J model*, Phys. Rev. B **48**, 550 (1993), and references therein.
- [23] P. W. Anderson, *Resonating valence bonds: A new kind of insulator?*, Mat. Res. Bull. **8**, 153 (1973); P. Fazekas and P. W. Anderson, *On the ground state properties of the anisotropic triangular antiferromagnet*, Philos. Mag. **30**, 23 (1974).
- [24] G. Baskaran, Z. Zou, P. W. Anderson, *The resonating valence bond state and high-T_c superconductivity—A mean field theory*, Solid state communications **63**, 973 (1987); P. W. Anderson, G. Baskaran, Z. Zou, and T. Hsu, *Resonating-valence-bond theory of phase transitions and superconductivity in La_2CuO_4 -based compounds*, Phys. Rev. Lett. **58**, 2790 (1987); G. Baskaran, and P. W. Anderson, *Gauge theory of high-temperature superconductors and strongly correlated Fermi systems*, Phys. Rev. B **37**, 580(R) (1988); G. Baskaran, *Resonating Valence Bond States in 2 and 3D: Brief History and Recent Examples*, Indian J. Phys. **89**, 583 (2006).
- [25] S. R. White, R. M. Noack, and D. J. Scalapino, *Resonating Valence Bond Theory of Coupled Heisenberg Chains*, Phys. Rev. Lett. **73**, 886 (1994).
- [26] S. A. Kivelson, D. S. Rokhsar, and J. P. Sethna, *Topology of the resonating valence-bond state: Solitons and high-T_c superconductivity*, Phys. Rev. B **35**, 8865 (1987); S. Liang, B. Doucot, and P. W. Anderson, *Some New Variational Resonating-Valence-Bond-Type Wave Functions for the Spin-1/2 Antiferromagnetic Heisenberg Model on a Square Lattice*, Phys. Rev. Lett. **61**, 365 (1988).
- [27] P. Monthoux, A. Balatsky, and D. Pines, *Weak-coupling theory of high-temperature superconductivity in the antiferromagnetically correlated copper oxides*, Phys. Rev. B **46**, 14803 (1992); S. Chakravarty, A. Sudbø, P. W. Anderson, and S. Strong, *Interlayer Tunneling and Gap Anisotropy in High-Temperature Superconductors*, Science **261**, 337 (1993).
- [28] R. Horodecki, P. Horodecki, M. Horodecki, and K. Horodecki, *Quantum entanglement*, Rev. Mod. Phys. **81**, 865 (2009).
- [29] M. Lewenstein, A. Sanpera, V. Ahufinger, B. Damski, A. Sen(De), and U. Sen, *Ultracold atomic gases in optical lattices: mimicking condensed matter physics and beyond*, Adv. Phys. **56**, 243 (2007); L. Amico, R. Fazio, A. Osterloh, and V. Vedral, *Entanglement in many-body systems*, Rev. Mod. Phys. **80**, 517 (2008).
- [30] A. Osterloh, L. Amico, G. Falci, and R. Fazio, *Scaling of entanglement close to a quantum phase transition*, Nature (London) **416**, 608 (2002); T. J. Osborne and M. A. Nielsen, *Entanglement in a simple quantum phase transition*, Phys. Rev. A **66**, 032110 (2002); G. Vidal, J. I. Latorre, E. Rico, and A. Kitaev, *Entanglement in Quantum Critical Phenomena*, Phys. Rev. Lett. **90**, 227902 (2003); L.-A. Wu, M. S. Sarandy, and D. A. Lidar, *Quantum Phase Transitions and Bipartite Entanglement*, Phys. Rev. Lett. **93**, 250404 (2004).
- [31] A. Kitaev and J. Preskill, *Topological Entanglement Entropy*, Phys. Rev. Lett. **96**, 110404 (2006); M. Levin and X.-G. Wen, *Detecting Topological Order in a Ground State Wave Function*, Phys. Rev. Lett. **96**, 110405 (2006); X. Chen, Z.-C. Gu, and X.-G. Wen, *Local unitary transformation, long-range quantum entanglement, wave function renormalization, and topological order*, Phys. Rev. B **82**, 155138 (2010).
- [32] T.-C. Wei, D. Das, S. Mukhopadhyay, S. Vishveshwara, and P. M. Goldbart, *Global entanglement and quantum criticality in spin chains*, Phys. Rev. A **71**, 060305(R) (2005); T. R. de Oliveira, G. Rigolin, M. C. de Oliveira, and E. Miranda, *Multipartite Entanglement Signature of Quantum Phase Transitions*, Phys. Rev. Lett. **97**, 170401 (2006); R. Orús, *Universal Geometric Entanglement Close to Quantum Phase Transitions*, Phys. Rev. Lett. **100**, 130502 (2008); M. Hofmann, A. Osterloh, and O. Gühne, *Scaling of genuine multipartite entanglement close to a quantum phase transition*, Phys. Rev. B **89**, 134101 (2014); A. Biswas, R. Prabhu, A. Sen(De), and U. Sen, *Genuine-multipartite-entanglement trends in gapless-to-gapped transitions of quantum spin systems*, Phys. Rev. A **90**, 032301 (2014).
- [33] H. S. Dhar and A. Sen(De), *Entanglement in resonating valence bond states: ladder versus isotropic lattices*, J. Phys. A: Math. Theor. **44**, 465302 (2011).

- [34] H. S. Dhar, A. Sen(De), and U. Sen, *The density matrix recursion method: genuine multisite entanglement distinguishes odd from even quantum spin ladder states*, New J. Phys. **15**, 013043 (2013); S. S. Roy, H. S. Dhar, D. Rakshit, A. Sen(De), and U. Sen, *Diverging scaling with converging multisite entanglement in odd and even quantum Heisenberg ladders*, New J. Phys. **18**, 023025 (2016).
- [35] H. S. Dhar, A. Sen(De), and U. Sen, *Characterizing Genuine Multisite Entanglement in Isotropic Spin Lattices*, Phys. Rev. Lett. **111**, 070501 (2013).
- [36] A. Chandran, D. Kaszlikowski, A. Sen(De), U. Sen, and V. Vedral, *Regional Versus Global Entanglement in Resonating-Valence-Bond States*, Phys. Rev. Lett. **99**, 170502 (2007).
- [37] R. Ramanathan, D. Kaszlikowski, M. Wiesniak, and Vlatko Vedral, *Entanglement in doped resonating valence bond states*, Phys. Rev. B **78**, 224513 (2008).
- [38] K. Sano, *Possible Phase Diagram of a t - J Ladder Model*, J. Phys. Soc. Jpn. **65**, 1146 (1996).
- [39] A. Sen(De) and U. Sen, *Channel capacities versus entanglement measures in multiparty quantum states*, Phys. Rev. A **81**, 012308 (2010); A. Sen(De) and U. Sen, *Bound Genuine Multisite Entanglement: Detector of Gapless-Gapped Quantum Transitions in Frustrated Systems*, arXiv:1002.1253 [quant-ph](2010). Also see Appendix.
- [40] A. Shimony, *Degree of entanglement*, Ann. NY Acad. Sci. **755**, 675 (1995); H. Barnum and N. Linden, *Monotones and invariants for multi-particle quantum states*, J. Phys. A **34**, 6787 (2001); M. Blasone, F. Dell'Anno, S. DeSiena, and F. Illuminati, *Hierarchies of geometric entanglement*, Phys. Rev. A **77**, 062304 (2008).
- [41] Another important derivation of the t - J model was obtained by Zhang and Rice from the three-band Hubbard model that describe the cuprate planes in high- T_c superconductors [42] (cf. [43]). The t - J model together with the one-band and three-band Hubbard models, in various limits, effectively describe the Hamiltonians for the study of high- T_c superconductivity, although disagreements exist [3, 4].
- [42] F. C. Zhang and T. M. Rice, *Effective Hamiltonian for the superconducting Cu oxides*, Phys. Rev. B **37**, 3759(R) (1988).
- [43] V. J. Emery and G. Reiter, *Quasiparticles in the copper-oxygen planes of high- T_c superconductors: An exact solution for a ferromagnetic background*, Phys. Rev. B **38**, 11938(R) (1988).
- [44] M. Ogata, M. Luchini, S. Sorella, and F. Assaad, *Phase diagram of the one-dimensional t - J model*, Phys. Rev. Lett. **66**, 2388 (1991); S. R. White and D. J. Scalapino, *Hole and pair structures in the t - J model*, Phys. Rev. B **55**, 6504 (1997); S. R. White and D. J. Scalapino, *Density Matrix Renormalization Group Study of the Striped Phase in the 2D t - J Model*, Phys. Rev. Lett. **80**, 1272 (1998); A. Moreno, A. Muramatsu, and S. R. Manmana, *Ground-state phase diagram of the one-dimensional t - J model*, Phys. Rev. B **83**, 205113 (2011); S. Guertler and H. Monien, *Unveiling the Physics of the Doped Phase of the tJ Model on the Kagome Lattice*, Phys. Rev. Lett. **111**, 097204 (2013).
- [45] M. Troyer, H. Tsunetsugu, and T. M. Rice, *Properties of lightly doped t - J two-leg ladders*, Phys. Rev. B **53**, 251 (1996).
- [46] G. Sierra, M. A. Martín-Delgado, J. Dukelsky, S. R. White, and D. J. Scalapino, *Dimer-hole-RVB state of the two-leg t - J ladder: A recurrent variational ansatz*, Phys. Rev. B **57**, 11666 (1998).
- [47] F. D. M. Haldane, *'Luttinger liquid theory' of one-dimensional quantum fluids. I. Properties of the Luttinger model and their extension to the general 1D interacting spinless Fermi gas*, J. Phys. C: Solid State Phys. **14**, 2585 (1981); N. Nagaosa and P. A. Lee, *Normal-state properties of the uniform resonating-valence-bond state*, Phys. Rev. Lett. **64**, 2450 (1990); C. A. Hayward and D. Poilblanc, *Luttinger-liquid behavior and superconducting correlations in t - J ladders*, Phys. Rev. B **53**, 11721 (1996).
- [48] A. Eckardt and M. Lewenstein, *Controlled hole doping of a Mott insulator of ultracold fermionic atoms*, Phys. Rev. A **82**, 011606(R) (2010).
- [49] S. Trebst, U. Schollwöck, M. Troyer, and P. Zoller, *d -Wave Resonating Valence Bond States of Fermionic Atoms in Optical Lattices*, Phys. Rev. Lett. **96**, 250402 (2006); A. M. Black-Schaffer and S. Doniach, *Resonating valence bonds and mean-field d -wave superconductivity in graphite*, Phys. Rev. B **75**, 134512 (2007).
- [50] Alternatively, several studies model the ground states of the doped t - J ladder, in the strong coupling regime, i.e., the exchange coupling along the rungs is much larger than any other parameter in the system, using a hole-dimer RVB composite state that allows the system to be mapped to a 1D hard core boson (HCB) Hamiltonian. The properties of the doped ladder system can then be described as a 1D Luther-Emery liquid with gapped spin excitations. For example, see Refs. [45, 46].
- [51] We develop a numerical algorithm, based on the Lanczos method [56], to exactly solve the composite hole-dimer qutrit system. By dividing the Hilbert space in different subspaces, according to the hole concentration and total S_z , exact ground state of the t - J Hamiltonian can be obtained for moderate system size. The algorithm is implemented using codes written in MatLab and Fortran90. Also, see the Appendix for more details.
- [52] R. F. Werner, *Quantum states with Einstein-Podolsky-Rosen correlations admitting a hidden-variable model*, Phys. Rev. A **40**, 4277 (1989).
- [53] E. H. Lieb and M. B. Ruskai, *Proof of the strong subadditivity of quantum-mechanical entropy*, J. Math. Phys. (N.Y.) **14**, 1938 (1973).
- [54] The counting of all possible dimer coverings with holes on a ladder configuration is not easily tractable using conventional exact methods. In fact, in a 2D quantum spin lattice, the arrangement of monomer and dimer coverings, as encountered in the doped RVB system, is NP-complete [37]. Also see, M. Jerrum, J. Stat. Phys. **48**, 121 (1987).
- [55] G. Sierra and M. A. Martín-Delgado, *Short-range resonating-valence-bond state of even-spin ladders: A recurrent variational approach*, Phys. Rev. B **56**, 8774 (1997).
- [56] C. Lanczos, *An Iteration Method for the Solution of the Eigenvalue Problem of Linear Differential and Integral Operators*, J. Res. Natl. Bur. Stand. **45**, 255 (1950); H. Nishimori, *Tipack-Numerical diagonalization routines and quantum spin Hamiltonians*, AIP Conf. Proc. **248**, 269 (1991).